



Fermilab

TM-1162
2126.000

CDF Note No. 150
January 20, 1983

MAGNETIC FIELD CALCULATION ON CDF DETECTOR (I)

R. Yamada

Fermi National Accelerator Laboratory
Batavia, Illinois 60510

I. Introduction

Magnetic field and flux distribution for the CDF detector is calculated using a TRIM program. The flux distribution in the system is calculated at several different excitation levels with an expected B-H curve.

The field uniformity inside the superconducting solenoid is plotted with deviation from the central field value for the axial and radial field components. The field distribution inside the conical region of the end plug is calculated and plotted. The fringing fields at the outside surfaces of the end plug and end wall, and the central hadron calorimeter are estimated, where the photo-multipliers will be installed.

The magnetic forces among the components of the CDF detector are calculated using its companion program FORGY. The total summation of axial force components for the whole system is compared with the estimation. There is some

difference between them and the errors are attributed to some components and the probable values are attributed to these components.

The effects of the change of B-H curve on the force of the coil and on the amount of flux going through the central calorimeter are estimated. Due to the uncertainty of the B-H curve, two extreme cases with extreme B-H curves were calculated and the resulting magnetic and mechanical parameters are compared. Also the field distribution without the central calorimeter is calculated.

There are about a dozen joints in the superconducting solenoid winding. The effect of these joints are estimated for the imaginary case with only one joint and for a more realistic case with eleven joints. In this case the effect of individual joints is relatively washed out due to the superposition of individual effects. The effect of iron skin plates over the end of the central electro-magnetic shower counter is also estimated.

Some of the magnetic field calculations for the CDF detector have been done for similar geometries,^{1,2} but the revised calculations with better results and other information are reported here.

II. Magnetic Geometry of CDF Detector

The magnetic structure of CDF detector, which is used for the field calculation, is shown in Fig. 1 (only a quadrant is shown). For the reason of simplicity the geometry is assumed completely axisymmetric, which is a justifiable assumption for our case.

The main difference between this model and the real detector is the structure of the back leg yoke. In reality the back-legs are composed of top and bottom lumped steel plates. They are far away from the central solenoid and are non-axisymmetric. For the calculation we have assumed perfect axisymmetry and have taken into account the non-symmetric yoke by using an effective width for the yoke of 10.7 inches, which gives the same cross sectional area. As a result the calculated field around the yoke should be regarded as an average value.

The CDF detector is not completely axisymmetric, but the main parts of the magnetic structure, including the central calorimeter, the end plug, the end wall, and the superconducting solenoid coil are axisymmetric. But both of the end wall and the central calorimeters at one end are composed of 24 modules each. There are 12 two inch thick reinforcing steel ribs in the end wall area, and both sides of an end wall module are covered by 1/8 inch thick iron plate skins. The central calorimeter modules have 3/16 inch thick iron plate skins. These iron plates will tend to

collect magnetic flux and may saturate locally.

The central calorimeter is composed of mostly one inch thick iron plates. But due to the limit of the available number of regions for the field calculation, it is assumed as a solid iron block. This is also a justifiable assumption, because the average flux density in it is fairly low.

In Fig. 1, the relative geometry of the iron plates for the calorimeters and the conductor for the coil is shown. The width of the actual superconductor is 3.3 mm ($=0.13$ "), but it is assumed one inch thick and the center is placed where the superconductor will be.

There are four reentrant pole pieces as shown in Fig. 1. They are placed to improve the magnetic field uniformity inside the solenoid and to reduce the axial force on the conductor. There is a one inch gap between the end-plug calorimeter and the end-wall calorimeter for the cables to go out. The thickness of the number 0 plate is changed from 2.5" to 0.5" at the radius of 79.5 inches to reduce the magnetic shunting to the central calorimeter.

III. Magnetic Field Calculation Program

A two dimensional magnetostatic program called TRIM³ was used to calculate the magnetic field distribution of the CDF magnet in the axi-symmetrical mode. Its accompanying subroutine FORGY⁴ was applied to estimate forces on the

calorimeters, the yoke and the coil. These programs are useful for axisymmetrical cases, but do not actually calculate in three dimensions.

The TRIM, which was used, is limited in the number of regions up to 100, and we cannot detail the structure of the central calorimeter as described before. It uses 680K memory and usually takes 30 minutes in the cpu time of the Argonne IBM 3033 computer.

The program is run in single precision due to the large number of mesh points, and the convergence is set at 10^{-5} . In our cases we found out that to get a converged result we had to fix the parameter RHOAIR, not to float it. Sometimes the value of 1.93 was used, below the recommended value of 1.94. Other times it was floated to find a value, corresponding to a minimum value of convergence but still not converged, and then its value is fixed in the second part of a run.

The following are recommendations for using these programs.⁵ It is recommended to make meshes close to square shapes, and to keep the ratio of side lengths of rectangular shaped meshes below one to four. We should use FOSSEDIT to calculate magnetic field strength from vector potential. To get results from FOSSEDIT the meshes lines should be rather straight. In order to get accurate values for forces in FORGY, the meshes on both sides of the boundary should be close to regular rectangular shapes. The coil width should

be at least three meshes wide.

IV. Flux Distribution in CDF Detector

The entire detector will be made of iron plates and slabs of possibly 1020 quality. These iron pieces are not excellent iron for magnetic structure, but inexpensive, usable and commercially readily available.

The used B-H curve for the calculation is based upon the data for the unannealed case of USS 1020 hot rolled carbon steel plates, up to 22 kG, which is the worst case of 1020 steel.⁶ Beyond 22 kG, the B-H curve was estimated from other sources. The composite B-H curve is shown in Fig. 2. In this figure the B-H curve for the other extreme iron, good iron, is also shown for comparison, which was also used.

The flux distribution in the CDF detector is shown in Fig. 3, which corresponds to 15 kG at center for the run "AE17 CDF". The detailed flux distribution around the end-plug and end-wall hadron calorimeters is shown in Fig. 4. The flux concentration is seen at the tip of the No. -4 plate and in the region, where No. 0, 1 and 2 plates have one inch gaps. At the highest place the flux density is estimated as high as 26.2 kG.

With this iron the flux density in the back leg is 10.9 kG. As is shown in Fig. 3, 11 flux lines out of a total of 50 lines go through the central calorimeter, and 23% of the total flux is going through the central calorimeter. Its

average flux density is about 0.91 kG.

In reality the central calorimeter is made of mostly 1" thick steel plates with 5/8" gap, with the space factor of about 62%. Therefore, the average flux density in the 1" plate will be about 1.5 kG. Also the first several steel plates near the coil will have much higher flux density, as can be guessed from Fig. 3.

If all parts of the cradle for the central calorimeter are made of iron, this will magnetically shunt the back leg yoke. Then it might introduce asymmetry for the flux distribution in the end-plug and end-wall calorimeters, causing some unbalance in the forces. It might be safer to put some non-magnetic material in this extra-magnetic path.

V. Field Uniformity inside Solenoid

The field uniformity inside the solenoid at 15 kG for Run "AE17 CDF" is shown in Fig. 5 and 6. In Fig. 5 the deviation ΔB_z of the axial field component from the central field $B_z(0)$ is shown in percent. The relative positions of the conductor winding and the boundary of the reentrant pole pieces are also shown. Inside the region for the central tracking chamber, the deviations are from +0.5% to -1% (corresponding to $Z = 0"$ to $Z = 44.5"$ to $59"$). In the region for the intermediate tracking chamber, the variation is from -0.5% to -4% (up to $Z = 68"$).

The axial field component is highest (+0.5%) near the central winding of the coil and gradually decreasing toward the opening of the pole-piece. Near the opening it decreases by 20 to 30%. This decrease is mainly due to the opening of the end-plug, and also due to the finite length of the solenoid winding. At both corners of the pole-piece the magnetic flux is seen to be concentrated.

The radial field component B_r for Run "AE17 CDF" at $B_z(0) = 15$ kG is shown in Fig. 6. It is normalized by the value of $B_z(0)$ and given in percent. The radially outward direction is taken positively. Along the conductor winding the radial component is growing up to 1% with increase of z up to 60 inches. This means the total flux is gradually leaking outwards in this region.

In the region for the intermediate tracking chamber the radial component is varying from +0.5% to 2%, corresponding to $B_r = 75$ to 300 Gauss, which will cause some problem for a TPC type chamber.

The value of H_c for the hot rolled carbon steel plates, not annealed, may be 4 oersteds or more. This may cause a residual field of about 10 Gauss, which is 0.7% of the central field. The uniformity in the field distribution due to this may be a few tenths of a percent.

VI. Field Distribution inside Hole of End-Plug

The field distribution inside the hole of the end-plug is shown in Fig. 7 and 8 for Run "AE17 CDF" at $B_z(0) = 15$ kG. In this calculation the outside boundary of the universe for the field calculation is taken at $Z = 200$ inches.

The axial and radial field components $B_z(z,r)$ and $B_r(z,r)$ are given in Fig. 7 and Fig. 8 respectively, both in units of Gauss. As the tip of the pole piece is at $r = 15.7$ ", the curves for $r = 4$ " and 15 " are always along in the air path. But parts of the curves for $r = 22$ ", 30 " and 42.5 " are going through the pole pieces, where the flux density in the iron plates are shown.

VII. Field Uniformity Optimization

The field shape around the end of the superconducting coil depends strongly on several factors, as will be discussed. To achieve the most uniform axial field distribution, it is preferable to put the end of the conductor layer as close to the yoke surface as possible. However, with a superconducting coil, some gap is required between coil and yoke for insulation and structure, which is different from a conventional coil. To improve the axial field uniformity, several reentrant steel plates (which act also as part of the end plug hadron calorimeter) extend into the bore of the coil.

To optimize the magnetic field uniformity and reduce the magnetic forces on the coil, the following major parameters can be adjusted. The numbers for the run "AE17 CDF" are added in parenthesis.

1. Number of the re-entrant iron plates in the coil bore (4 plates).
2. Axial gap between the end of the superconducting conductor and the surface (5.70 inches/145 mm).
3. Radial gap between the re-entrant iron plates and the superconducting conductor (3.38 inches/86 mm).
4. B-H curves of iron plates. (Bad 1020 iron)

VIII. Electromagnetic Forces on Detector Components

There are five major components of the CDF detector which are affected by the magnetic forces. They are the superconducting solenoid coil itself, the end plug, calorimeter, the end wall calorimeter, the yoke, and the central calorimeter. A half of the whole detector system is considered and the forces are given for the corresponding half components.

Force on Coil. The force on the coil during magnetic excitation has been studied. There are two force components. One is the radial component which corresponds to a magnetic pressure of about 130 psi (9 kg/cm^2), and the other is an axial force component caused by the radial component of the fringing field at the end of the conductor. This axial force can be minimized by choosing the optimum

iron/coil geometry. The calculated "AE17 CDF" case has an axial force of -100.2×10^4 N (-102.2 metric tons) toward the coil midplane. The forces from both ends of the coil compress the coil but do not result in a net force on the coil if the coil is axially centered in the iron yoke.

Force on End Plug. The end plug hadron calorimeter is made of a stack of 2 inch thick washer-shaped iron plates. The end plug is pulled as a unit into the center of the coil during magnet excitation. The total inward force calculated for "AE17 CDF" is -528×10^4 N (539 metric tons) with correction for each end plug. The distribution of the total force on individual plates is shown in Table II for "AE17 CDF" case. Interestingly the innermost re-entrant plates are not being pulled inwards strongly, because they are in a nearly uniform field. The plate No. -4 is rather pushed outward. The radial forces on these plates are also shown in the table.

Force on End Wall. The forces on the end wall calorimeter, which is also made of two inch thick iron plates, are also listed in Table II. Only the second and the third plates are being pulled inwards. The remaining plates are being pushed moderately outward. The total outward force is 12.4×10^4 N (12.6 metric tons), for the total structure of the end wall calorimeter. There are two inch thick structural iron plates and 1/8 inch thick skin plates perpendicular to the two inch plates for the end wall

calorimeter. They were not taken into account in the field calculation, and will cause some change in the force on the end wall calorimeter.

The radial force on the end wall is also listed in Table II. As is expected, its total radial force of -305.8×10^4 N (-311.9 metric tons), matches that of the end plug $+307.2 \times 10^4$ N ($+313.3$ metric tons).

Force on Central Calorimeter. The forces on the central calorimeter are also listed in Table II. The total radial inward force is 2.19×10^4 N (2.23 metric tons) corresponding to roughly 93 kg/15° unit. The axial force is 2.76 metric tons toward the end wall calorimeter for the 2.5 m long circular assembly. Thus, these forces on the central calorimeter can be easily handled.

IX. Total Axial Force

The axial forces on these four components and the back leg yoke for "AE17 CDF" adds to 543.5×10^4 N without correction as shown in Table I. While the total Maxwell stress F_M in the median plane can be calculated from the area of the coil and the central field $B = 14.939$ kG, and we get $F_M = 612.7 \times 10^4$ N (625 metric tons). From the law of conservation of total force in a closed system, these two numbers should be the same. The added number is about 88.7% of F_M value, and the missing force of 69.2×10^4 N is most probably due to the calculational approximation in the

program. As explained in the next chapter it is most reasonable to attribute the difference to the possible errors in the axial forces of the end-plug plates and increase them accordingly. The corrected forces are given in Table II, which differs from Table I only in the values of the axial forces of the end plug.

The total amount of the axial force is conserved. Therefore, if the axial force of the coil is increased due to some geometrical change of iron structure, the remaining axial force on other components is decreased.

X. Consideration for Correction of Axial Forces

In the program FORGY, the force on the coil \mathbf{F} is calculated directly from the equation

$$\mathbf{F} = I \int (d\mathbf{S} \times \mathbf{B}),$$

where \mathbf{B} is a magnet fringing field at the conductor.

The axial forces on the central calorimeter and the yoke are rather small, and they are derived directly from the surface magnetic charge density on the surface.

The axial force components of the end plug and the end wall calorimeters are derived similarly from the surface magnetic charge. But they are made of thin iron plates, which are placed in strong magnetic field. Therefore the net axial force component of each plate is derived by the

summation of all components from all three or four surfaces. There are usually two big axial components with iron plates for the end-plug, which are opposing in their directions. As an example the detailed force components on plate No. 1 is given in Table III. The net force is about 20% of the big components. As the net force is determined with an accuracy of 10%, then the individual force components are calculated with the accuracy of 2%. To achieve an accuracy better than this seems hard in our case.

As can be seen from Fig. 3, the plates for the end-plug calorimeter are traversed by the magnetic flux much more than those of the end-wall calorimeter. Therefore, we apply the necessary correction for the missing axial force, only to the end-plug.

The general accuracy of the force calculation by the program FORGY is supported by the data for the total radial force as shown in Table II. In this case, the missing force is about 0.1% of the radial force on the end plug. For this summation the radial force on the coil is neglected, because its radial force is counter-balanced by its hoop stress.

XI. Total Axial Forces and Excitation Field

The total amount of the axial force on the coil is calculated at different current levels for the bad 1020 iron case, and at 15 kG for the good iron. They are shown in Fig. 9 and summarized in Table IV. It is shown that the

axial force of the coil is increasing roughly proportionally to the 2.6 power of the central magnetic field from 5 to 15 kG. This shows that the fringing field, which causes the axial force on the coil, is increasing relative to the central field. The force at 15 kG is about 5% higher with the bad 1020 iron compared with the good iron.

The total axial forces on the whole detector system at 10 and 15 kG are also shown in Table IV and Fig. 9, where this total is shown roughly proportional to the square of the central field B_0 .

References

1. R. Fast et al. Fermilab Internal Report TM-1075, Oct. 1981.
2. R. Fast et al. Fermilab Internal Report TM-1135, Oct. 1982.
3. R. J. Lari and J. K. Wilhelm, Computer Program TRIM for Magnet Design, Argonne Internal Report, unpublished (May 22, 1972).
4. T. K. Khoe and R. J. Lari, "FORGY" A Companion Computer Program of "TRIM" to Calculate Forces and Energy in Electromagnets, Argonne Internal Report, unpublished (January 4, 1972).
5. R. J. Lari - private communication.
6. "Non-oriented Electrical Steel Sheets Manual", p. 212, United States Steel.

Table I FORCES ON END PLATES (UNCORRECTED)

RUN NO = AE-17 B(KG) = 15 BO(KG) = 14.939
B-H CURVE = BAD1020 CONVERGENCE = 9.46E-06

PLATE NO	END PLUG		END WALL	
	FR	FZ	FR	FZ
	RADIAL FORC/PLT (X10 ⁴ N)	AXIAL FORC/PLT (X10 ⁴ N)	RADIAL FORC/PLT (X10 ⁴ N)	AXIAL FORC/PLT (X10 ⁴ N)
REENTRANT				
-4	0.854	19.326		
-3	4.479	-19.44		
-2	15.481	-33.86		
-1	17.85	-38.848		
REGULAR				
0	37.672	-73.153	-48.65	3.323
1	33.444	-72.569	-49.096	-12.579
2	42.623	-48.021	-46.589	-3.123
3	39.551	-48.618	-42.178	1.639
4	34.198	-41.896	-35.204	5.573
5	25.76	-37.164	-27.652	4.994
6	19.558	-25.434	-19.007	4.266
7	11.717	-15.344	-12.918	3.38
8	8.149	-8.834	-7.999	1.413
9	5.001	-5.693	-5.435	1.338
10	3.468	-3.488	-3.45	0.49
11	2.293	-2.288	-2.495	0.628
12	1.702	-1.458	-1.722	0.351
13	1.306	-1.05	-1.358	0.351
14	1.08	-0.679	-1.169	0.332
15	1.011	-0.327	-0.886	0.031
TOTAL	307.207	-458.829	-305.8	12.415

SUMMARY ON FORCE

AXIAL FORCES ON SYSTEM

COIL -100.18
END PLUG -458.829
END WALL 12.415
YOKE 0.427
CNT-CALO 2.701

TOTAL AXIAL -543.465 X10⁴ NEWTONS

TOTAL MAXWELL STRESS IN MEDIAN PLANE

612.702 X10⁴ NEWTONS

BALANCE=TOTAL AXIAL FORCE/MAXWELL STRESS

88.699 %

RADIAL FORCES ON SYSTEM

END PLUG 307.207
END WALL -305.8
YOKE 0.508
CNT-CALO -2.167

TOTAL RADIAL -0.271 X10⁴ NEWTONS

Table II FORCES ON END PLATES (CORRECTED)

18

RUN NO = AE-17 B(KG) = 15 BO(KG) = 14.939
 B-H CURVE = BAD1020 CONVERGENCE = 9.46E-06

PLATE NO	END PLUG		END WALL	
	FR	FZ	FR	FZ
	RADIAL FORC/PLT (X10 ⁴ N)	AXIAL FORC/PLT (X10 ⁴ N)	RADIAL FORC/PLT (X10 ⁴ N)	AXIAL FORC/PLT (X10 ⁴ N)
REENTRANT				
-4	0.854	22.242		
-3	4.479	-22.374		
-2	15.481	-38.969		
-1	17.85	-44.71		
REGULAR				
0	37.672	-84.192	-48.65	3.323
1	33.444	-83.52	-49.096	-12.579
2	42.623	-55.268	-46.589	-3.123
3	39.551	-55.955	-42.178	1.639
4	34.198	-48.218	-35.204	5.573
5	25.76	-42.773	-27.652	4.994
6	19.558	-29.272	-19.007	4.266
7	11.717	-17.659	-12.918	3.38
8	8.149	-10.167	-7.999	1.413
9	5.001	-6.552	-5.435	1.338
10	3.468	-4.014	-3.45	0.49
11	2.293	-2.633	-2.495	0.628
12	1.702	-1.678	-1.722	0.351
13	1.306	-1.208	-1.358	0.351
14	1.08	-0.781	-1.169	0.332
15	1.011	-0.377	-0.886	0.031

TOTAL	307.207	-528.067	-305.8	12.415

SUMMARY ON FORCE

AXIAL FORCES ON SYSTEM

COIL -100.18
 END PLUG -528.067
 END WALL 12.415
 YOKE 0.427
 CNT-CALO 2.701

TOTAL AXIAL -612.703 | X10⁴ NEWTONS

TOTAL MAXWELL STRESS IN MEDIAN PLANE
 612.702 X10⁴ NEWTONS

BALANCE=TOTAL AXIAL FORCE/MAXWELL STRESS
 99.999 %

RADIAL FORCES ON SYSTEM

END PLUG 307.207
 END WALL -305.8
 YOKE 0.508
 CNT-CALO -2.187

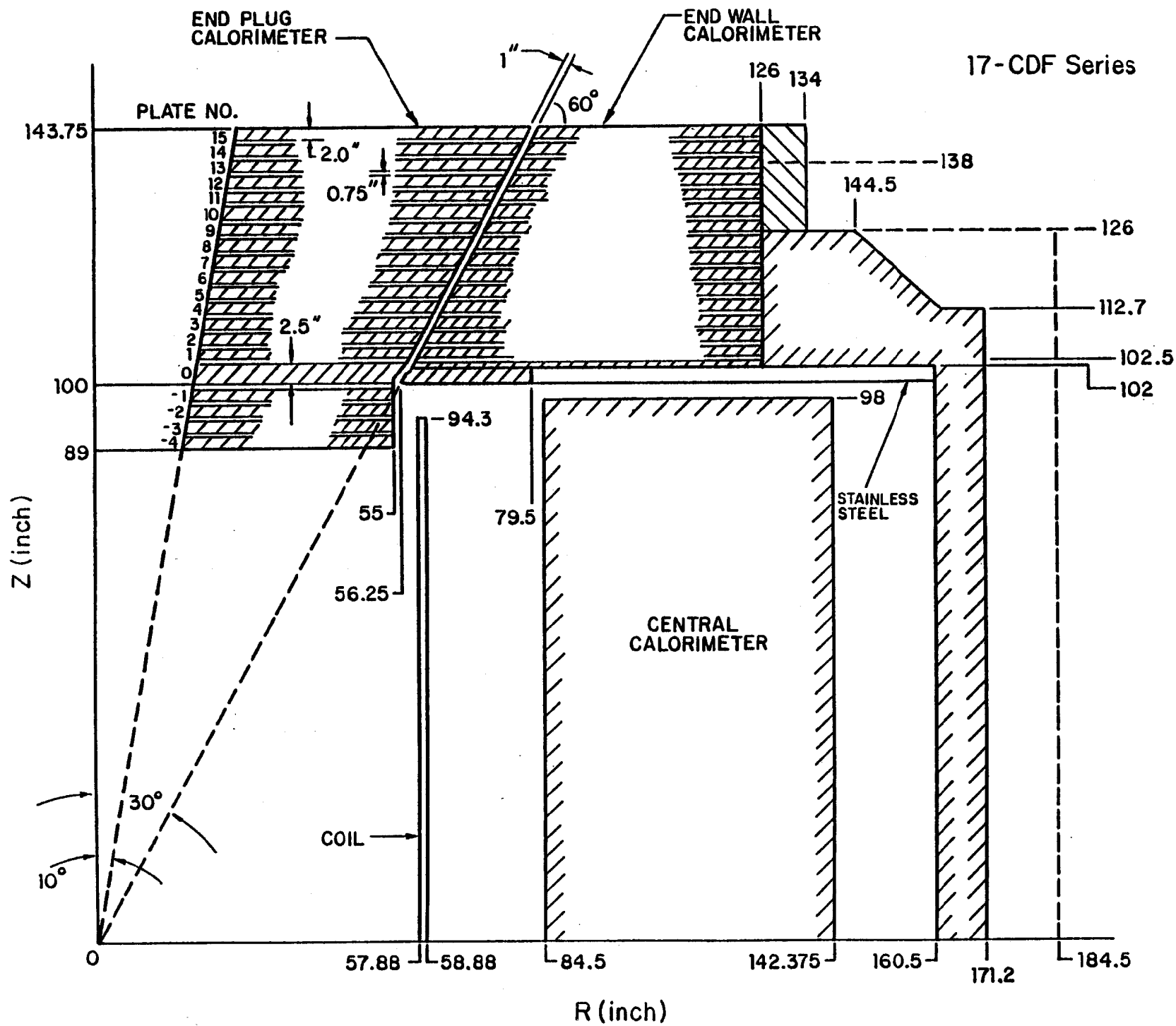
TOTAL RADIAL -0.271 X10⁴ NEWTONS

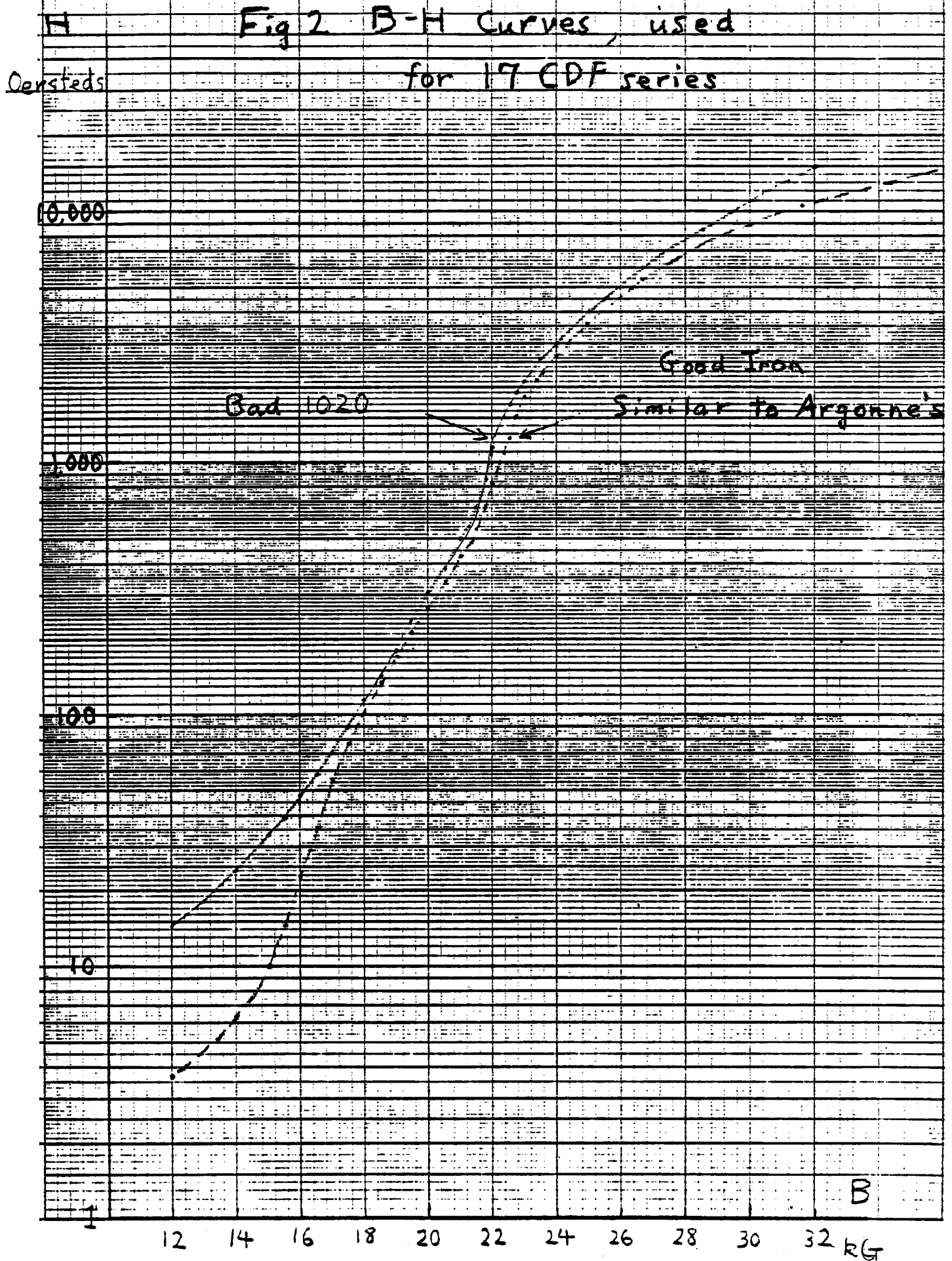
Table III. Detailed Force Components for No. 1 Plate of End-Plug Calorimeter, at 15 kG for Run "AE17-CDF" (uncorrected data)

Side	Radial Force ($\times 10^4$ N)	Axial Force ($\times 10^4$ N)
Bottom	- 7.376	-376.729
Top	- 2.312	+314.998
Inner Radius	+ 0.232	- 0.521
Outer Radius	+42.900	- 10.317
Net	+33.444	- 72.569

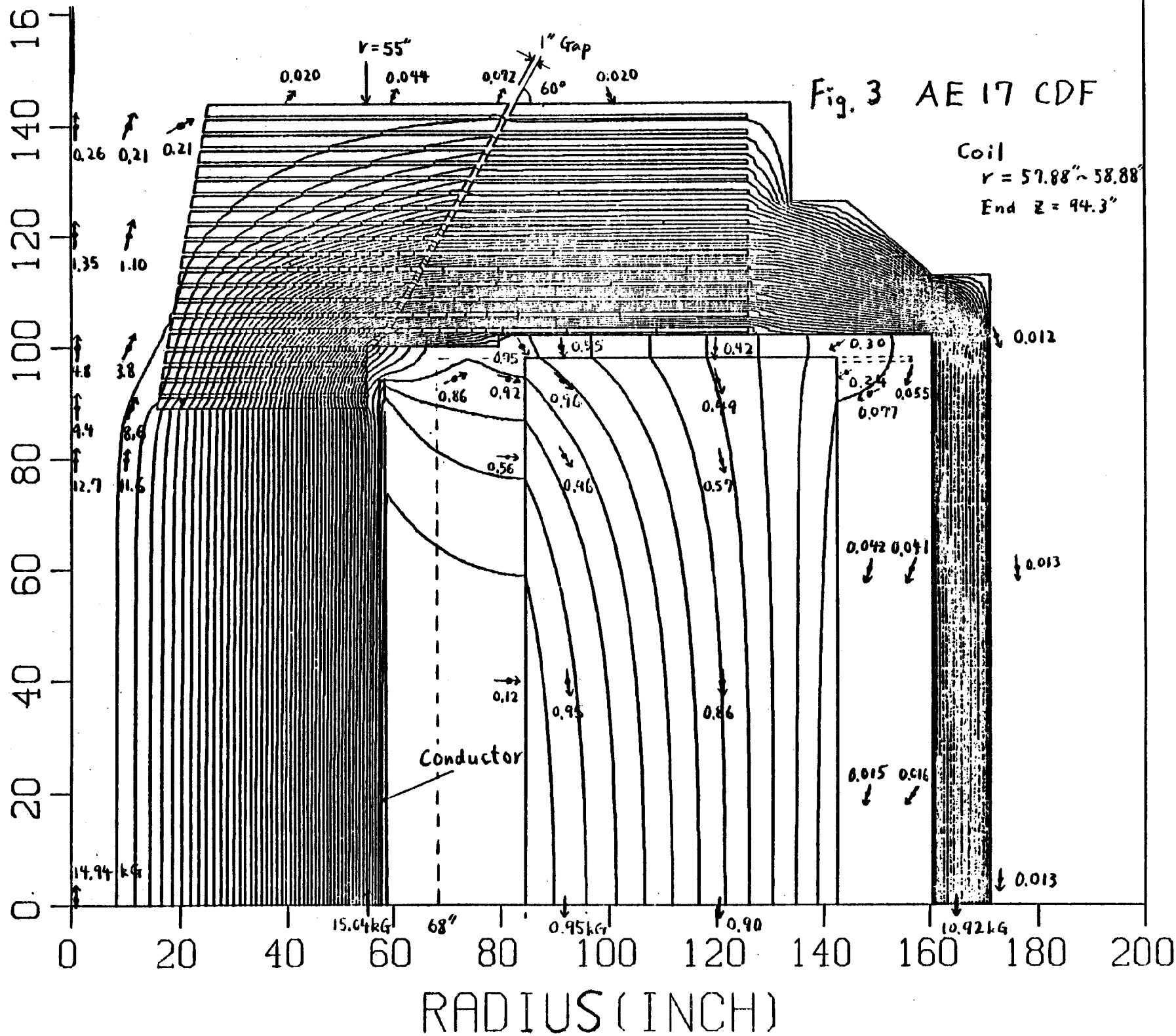
Table IV. Excitation Field and Total Azimuthal Forces on Coil and Whole Detector

Central Field B(kG)	BH-Curve	Total Axial Force on Coil $\times 10^4$ N	Uncorrected Total Axial Force on Whole Detector $\times 10^4$ N
5	Bad 1020	- 5.95	
10	Bad 1020	- 32.57	-244.50
13.5	Bad 1020	- 73.59	
15	Bad 1020	-100.18	-543.47
15	Good	- 94.73	-542.95
15	Bad 1020 without central calorimeter	- 86.14	





Z (INCH)



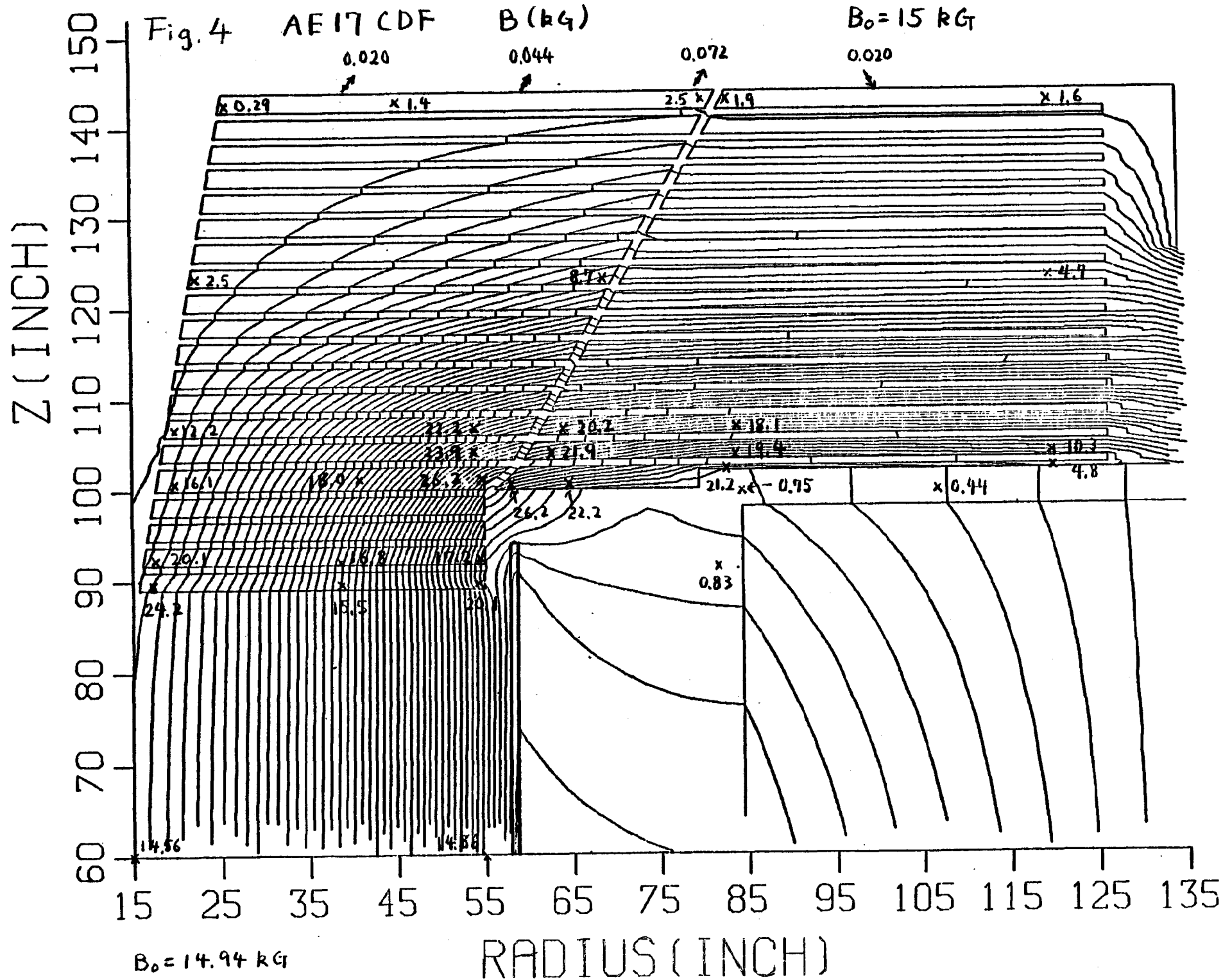


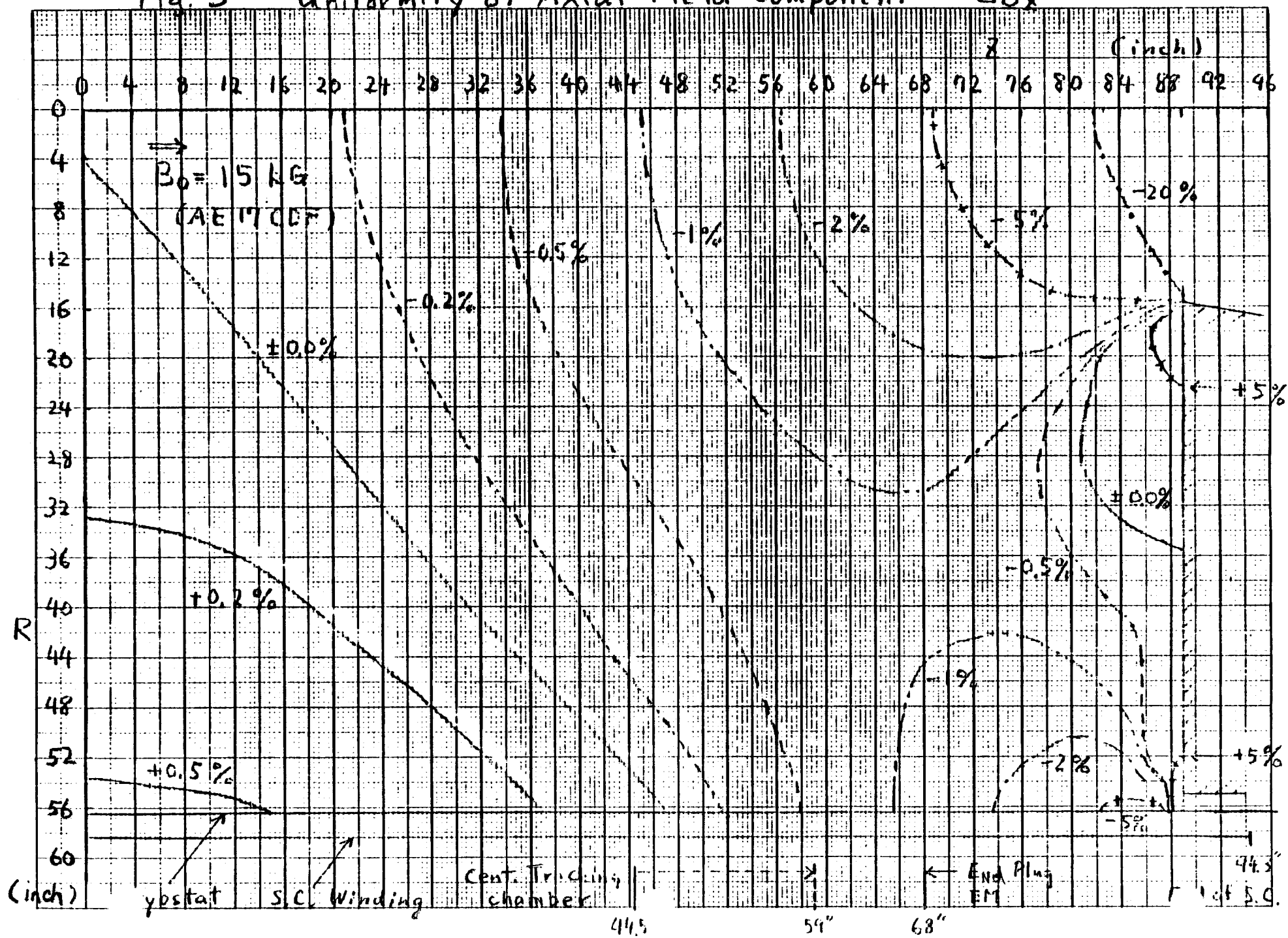
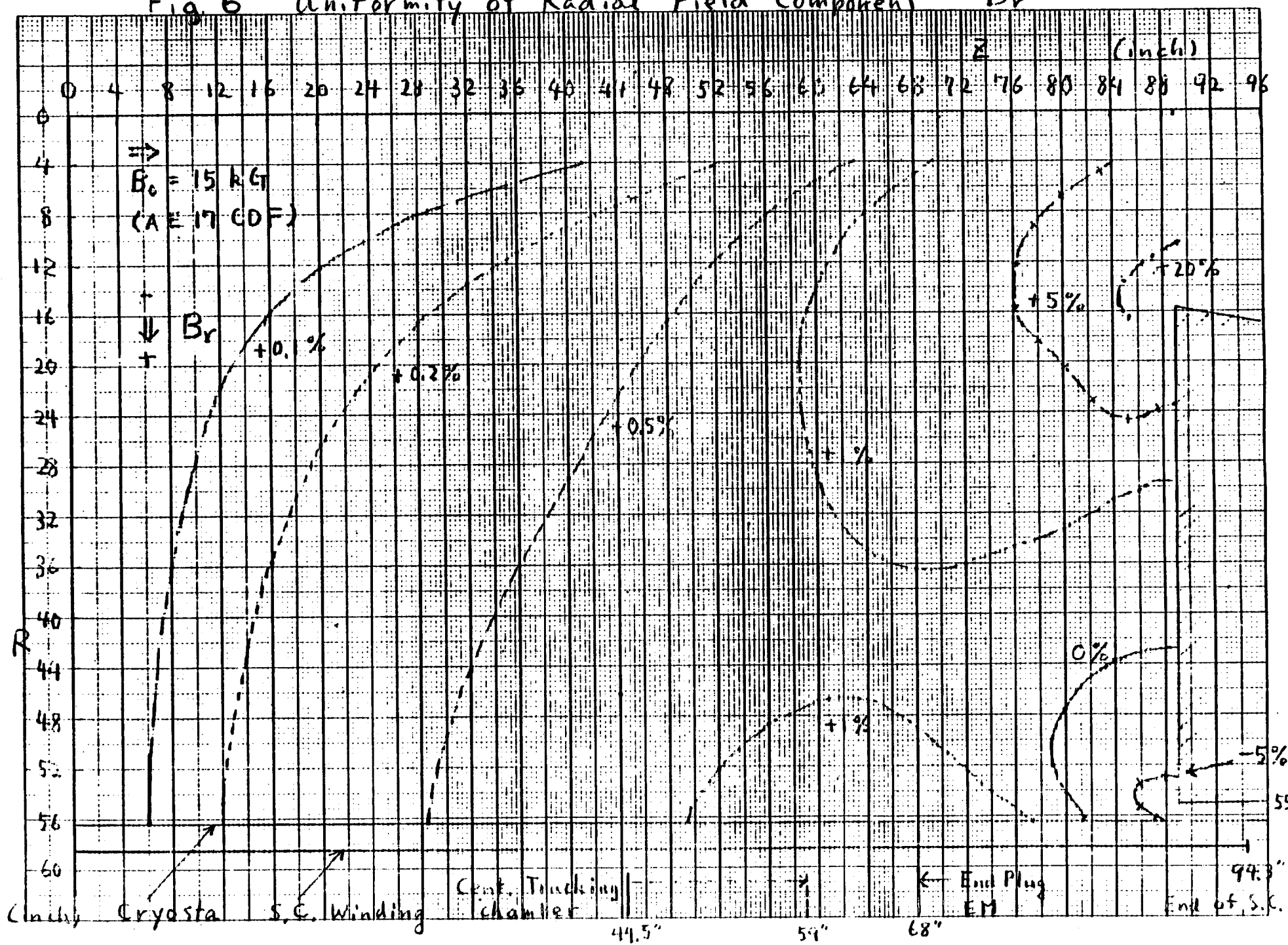
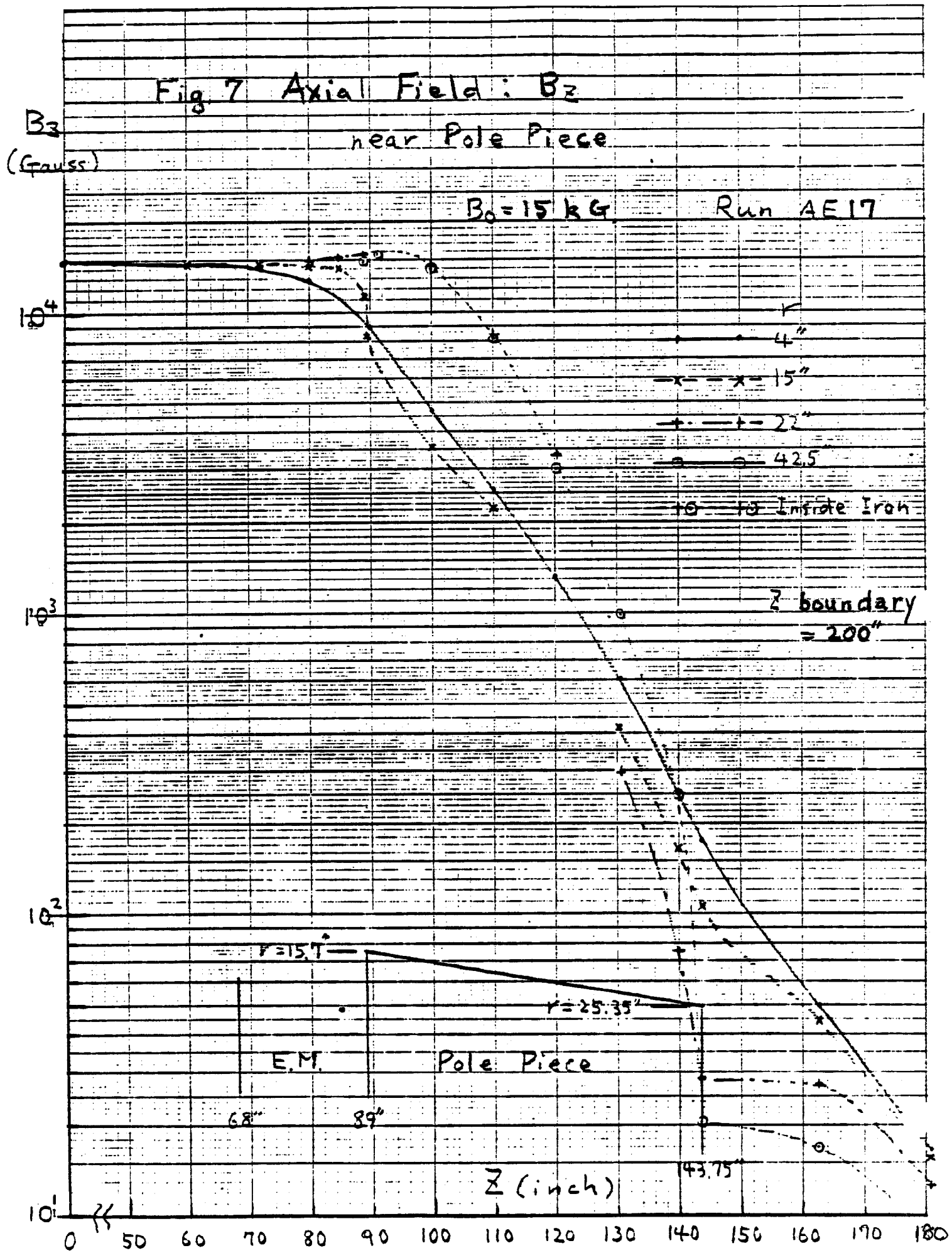
Fig. 5 Uniformity of Axial Field Component ΔB_z 

Fig 6 Uniformity of Radial Field Component B_r





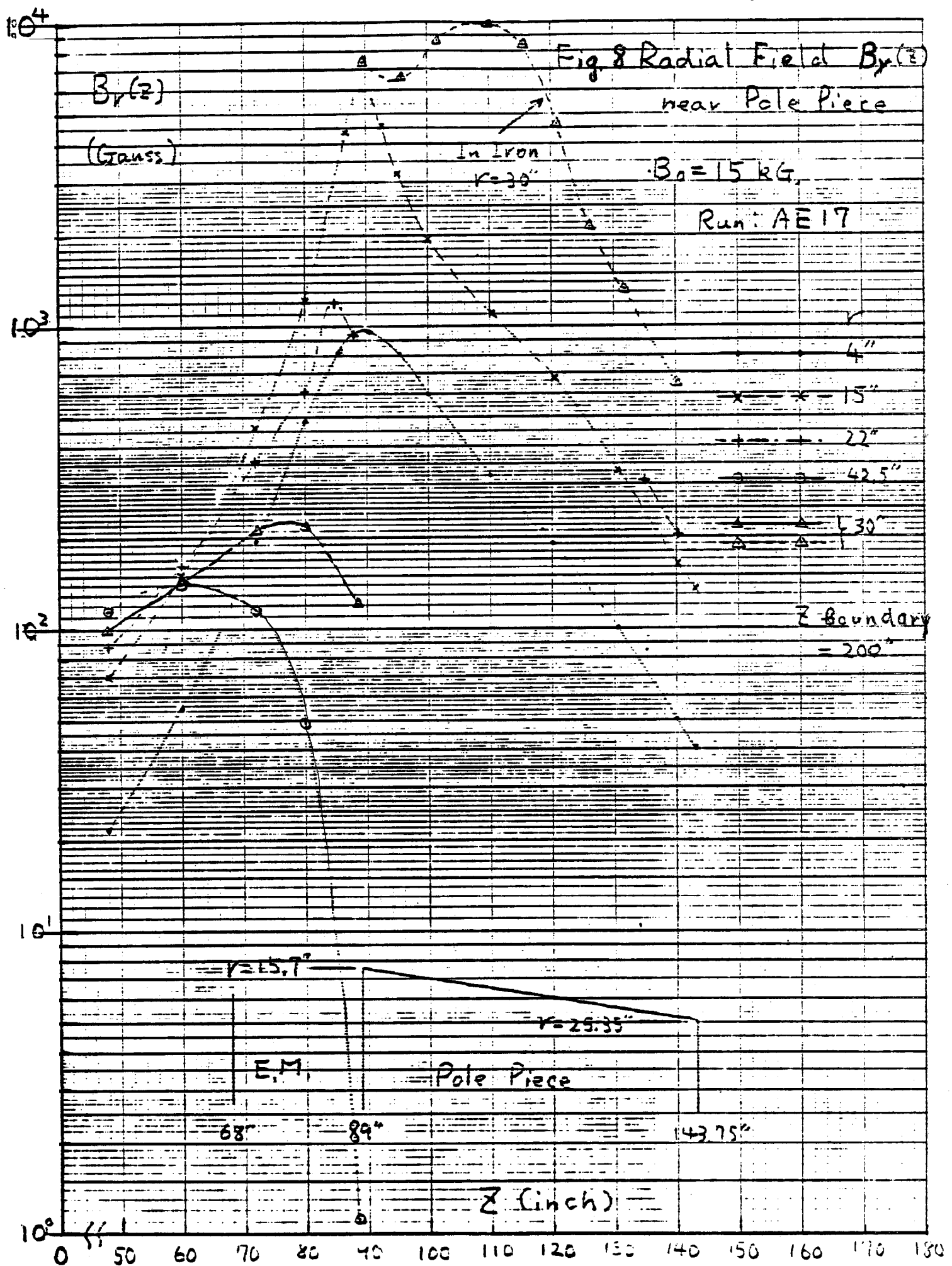


Fig. 9 Total Axial Forces on Coil

and Whole System

